27

Application of Electrochemical Impedance Spectroscopy (EIS) and X-ray Photoelectron Spectroscopy (XPS) to the Characterization of RTILs for Electrochemical Applications

J. Benavente[1] and E. Rodríguez-Castellón[2]
[1]*Grupo de Caracterización Electrocinética en Membranas e Interfases. Departamento de Física Aplicada I. Facultad de Ciencias. Universidad de Málaga*
[2]*Departamento de Química Inorgánica. Facultad de Ciencias. Universidad de Málaga. Spain*

1. Introduction

Ionic liquids (ILs) are low temperature molten salts, that is, a salt in the liquid state. ILs used to present a very low vapour pressure and this property makes of the ILs key materials for the development of a wide variety of emerging technologies. The stability of ILs at high temperatures (several hundred degrees), low combustibility, and even the relatively high viscosity of some of them compared to conventional solvents, are characteristic of interest for some applications. Due to the large diversity of ILs components, they may present wide structural variations which can be used to design the IL with more adequate properties for a particular application. These applications might include new types of lubricants and fluids for thermal engines, electrodeposition, energy and CO_2 capture devices, biomimetics, double layer capacitors,…..in fact, the scientific and technological importance of the ILs spans nowadays to a wide range of applications [1-5].

Among the energy devices, polymer-electrolyte membranes for fuel cell application are under development as a way to reduce global warming and energy cost and ILs incorporation in the structure of Nafion, a typical membrane for fuel cell use, is under study [6-8]. Since transport properties of porous and dense membranes can be modified with the addition of substances which could favour/reject the pass of some of the particles or ions in a mixture, the incorporation of a particular IL in the structure of a membrane may increase its selectivity and/or specificity.

Chemical characterization and determination of electrical parameters for different ILs as well as the changes associated to water incorporation, a subject of interest for different electrochemical applications, is considered in this work. Moreover, due to the importance that membrane separation technology has nowadays, modification of membranes with different structures by incorporation of RTILs or IL-cations and their effect on mass and charge transport is also presented.

Ionic liquids, membranes and membranes/IL-modified samples were chemically characterized by X-ray photoelectron spectroscopy (XPS). This technique allows the

determination of the surface chemical composition of a given sample and other properties related to the structure and chemical environment in which the atom lies within the solid and, in the case of membranes, it is commonly used to study chemical changes in polymer matrix [9-11]. Impedance spectroscopy (IS) measurements were performed for electrical characterization of both ILs and IL-modified membranes by analyzing the impedance plots and using equivalent circuits as models [12-16]. Time evolution of the IS plots was used as a way for monitoring both water diffusion in the ILs and IL inclusion in the membranes (or its loose from them), but also to show interfacial effects depending on the external conditions of the studied systems. Moreover, a comparison of the electrochemical parameters (ion transport numbers, water diffusion coefficient, electrical resistance and capacitance) obtained for fresh and aged samples of a IL-supported membrane or for original and IL-modified cellulosic membranes is also presented as examples of the interest of the studied systems and potentiality of the techniques used.

2. Experimental

2.1 Ionic liquids

The following room temperature ionic liquids were studied: 1-*n*-butyl-3-methylimidazolium hexafluoro-phosphate or [C_4MIM^+][PF_6^-]; 1-*n*-octyl-3-methylimidazolium hexafluoro-phosphate or [C_8MIM^+][PF_6^-], 1-*n*-decyl-3-methylimidazolium tetrafluoroborate or [$C_{10}MIM^+$][BF_4^-], 1-*n*-butyl-3-methylimidazolium tetrafluoroborate or [$BMIM^+$][BF_4^-] and n-dodecyltriethylammonium chloride or [DTA^+][Cl^-]. Both commercial (Solchema, Portugal) and prepared ILs following reported procedures [17-19] were used; in the case of the [DTA^+][Cl^-] (solid at room temperature) a 40% (w/w) solution with deionised water was prepared.

2.2 Membranes

The electrochemical characterization of the RTILs-modified membranes was performed with different kinds of flat membranes with porous and dense structure: i) a porous polyvinylidene fluoride (PVDF) membrane (FP-Vericel, Pall, USA) with nominal pore size of 0.2 μm and a thickness of 125 μm; ii) a dense perfluorinated proton-exchange Nafion-112 membrane in protonated form from Dupont, USA; iii) a dense but highly hydrophilic cellulosic membrane with 0.06 kg/m² of regenerated cellulose (sample RC-6) from Cellophane Española, S.A. (Burgos, Spain).

The supported liquid membrane (SLM) was obtained placing the PVDF porous support in a desiccator under vacuum for 1 hour, then (still under vacuum) the ionic liquid was released onto the membrane surface from a syringe (100 μl of ionic liquid per cm² of membrane area). The SLM is named by the RTIL used for its preparation and a detailed explanation of SLM preparation is presented in ref [11].

ILs incorporation into the structures of two dense membranes was performed by contacting the membranes with aqueous solutions of the ILs for different periods of time. A Nafion-112 membrane (Dupont, USA) was placed in the test-cell B (see Fig. 1) and both half-cell were filled with a 40% (w/w) aqueous solution of [DTA^+][Cl^-] and cation incorporation into the Nafion structure was obtained by proton-exchange (H^+/DTA^+) according to previous studies [20], while a piece of the hydrophilic cellulosic membrane was immersed for 1 week in a 50 % water solution of [$BMIM^+BF_4^-$] and dried at room temperature conditions for another week; these ILs-modified membranes will be hereafter named as Nafion/DTA and CR-6/$BMIMPB_4$, respectively.

2.2 X-ray photoelectron spectroscopy (XPS) measurements

[C_8MIM^+][PF_6^-], [C_8MIM^+][PF_6^-] and [$C_{10}MIM^+$][BF_4^-] RTILs and the surfaces of the original and IL-modified membranes were chemical characterized by XPS analysis. The high-resolution spectra were recorded with a Physical Electronics PHI 5700 spectrometer by using a concentric hemispherical analyzer operating in the constant pass energy mode at 29.35 eV, with 720 μm diameter analysis area, and MgK_α X-ray as an excitation source ($h\nu$ = 1253.6 eV). Accurate ±0.1 eV binding energies were determined with respect to the position of the adventitious C 1s peak at 284.8 eV, and the residual pressure in the analysis chamber was maintained below 5 x 10^{-7} Pa during data acquisition. A PHI ACCESS ESCA-V6.0F software package was used for acquisition and data analysis [21]. Atomic concentration (A.C.) percentages of the characteristic sample elements were determined after subtraction of a Shirley-type background taking into account the corresponding area sensitivity factor [22] for the different measured spectral regions. In the study performed with original and ILs- modified membranes, an irradiation time less than 20 minutes was used to minimize possible X-ray induced damage in the polymer structure [23].

2.3 Impedance spectroscopy measurements

Two slightly different test cells were used for impedance spectroscopy (IS) measurements carried out with different ILs and membrane/electrolytes (ILs or NaCl aqueous solutions) systems. Fig. 1 shows a scheme of the two open electrochemical cells used for electrochemical characterization, which consist of two glass semi-chambers with one

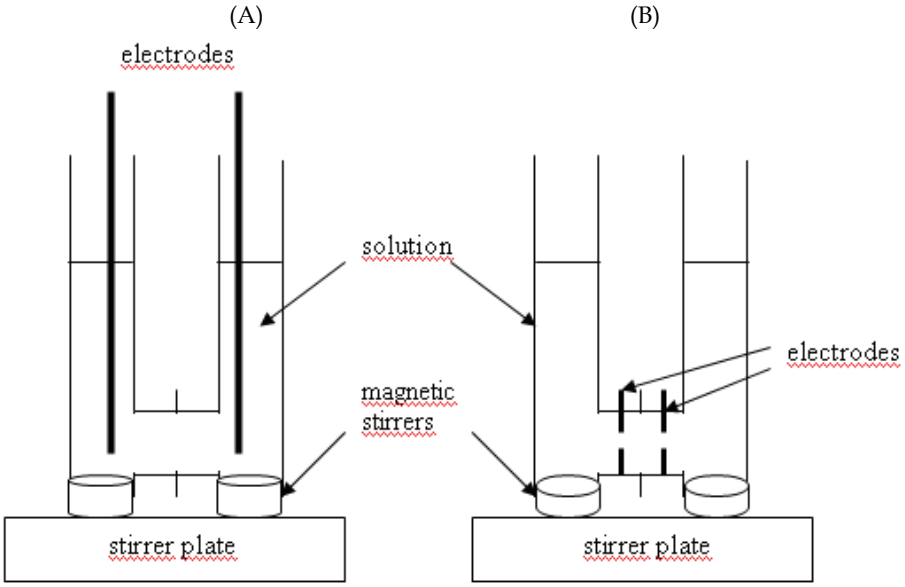

Fig. 1. Test cells for impedance spectroscopy and membrane potential measurements. In the case of RTILs and NaCl solutions both semi-cameras (in cells A or B) are filled with the electrolytes, while membranes are placed in the middle of the semi-cameras for membrane characterization.

electrode in each one, which were located in position (A) or position (B). The main difference between both cells is the direct contact between the electrode and the liquid open surface for test-cell A, which does not exist in the case of test-cell B. IS measurements were carried out with both semi-cell were filled with the studied RTILs.
Membrane electrical characterization was performed in test-cell A, with the membranes placed between both chambers supported by rubber rings and ILs or NaCl solutions filling both half-cells (electrode/electrolyte/membrane/electrolyte/electrode system) [16]. In the case of dry samples, the test-cell consists of a Teflon support on which two Pt electrodes were placed and screwed down (system electrode/membrane/electrode). In all cases, the electrodes were connected to a Frequency Response Analyzer (FRA, Solartron 1260) and measurements were recorded for 100 data points with a frequency ranging between 1 Hz and 10^7 Hz, at a maximum voltage of 0.01 V. Impedance data were corrected by parasite capacitances.

2.4 Electrochemical characterization of membranes.

Membrane potential (MP) measurements were performed in test-cell A using aqueous NaCl solutions and reversible Ag/AgCl electrodes connected to a high impedance voltmeter (Yokohama 7552, 1GΩ input resistance). The concentration of the NaCl solution was kept constant at one side of the membranes (c_c = 0.01 M), while the concentration of the NaCl solution at the other membrane side (c_v) was gradually changed from 0.002 M to 0.1 M [24].
Water diffusion coefficient through RC-6 and RC-6/BMIM membranes was determined by diffusion experiments with tritiated water (TOH) carried out in-cell A. One of the half-cells (donor chamber) contained 30 μl tritium/15 mL of distilled water while the other half-cell (receiving chamber) was filled with distilled water at t = 0; time variation of the tritium activity in the donor and receiving chambers was determined at different time instances by taken samples of 50 μl which were analyzed in a Beckman LS6500 scintillation counter [25].

3. Results and discussion

3.1 Electrical and chemical characterizations of ionic liquids.

Electrical characterization of pure and water-containing ILs was carried out by analyzing the impedance spectroscopy (IS) plots obtained for medium range frequencies (between 1 Hz and 10 MHz). IS is a non-destructive a.c. technique for electrical characterization of solid and liquid systems, but it can also be used for the determination of interfacial effects [16].
When a linear system is perturbed by a small alternating voltage $v(t) = V_o \sin\omega t$, its response, the electric current is also a sine wave, $i(t) = I_o \sin(\omega t+\phi)$, where V_o and I_o represent the maximum voltage and intensity, respectively, while $\omega=2\pi f$ is the angular frequency and ϕ the phase angle. A transfer function, the admittance function, can be defined as: $Y^*(\omega) = |Y(\omega)|e^{j\phi}$, where $|Y(\omega)|$ represents the amplitude, and the impedance function, $Z(\omega)$, is the inverse of the admittance: $Z(\omega)=[Y^*(\omega)]^{-1}$; the impedance is expressed as a complex number: $Z = Z_{real} + j\, Z_{img}$, where Z_{real} and Z_{img} are the real and imaginary parts of the impedance, respectively. The admittance for a parallel resistance-capacitor (RC) circuit is given by the sum of conductance (1/R) and capacitance (C) contributions, where the resistance (R) represents the dissipative component of the dielectric response while the capacitance describes the storage component. The impedance function for that circuit is: $1/Z^* = (1/R) + (j\omega C)$, and it can be separated into real and imaginary parts by algebra rules, which are related with the electrical parameters of the system by the following expressions:

$$Z_{real} = (R/[1 + (\omega RC)^2]) \; ; \qquad Z_{img} = - (\omega R^2 C/[1 + (\omega RC)^2]) \tag{1}$$

These expressions correlate impedance components, which are determined from experimental values using impedance plots, with the electrical parameters of the system.
The analysis of the impedance data can be carried out by the complex plane method by using the Nyquist plot ($-Z_{img}$ vs Z_{real}). The equation for a parallel (RC) circuit gives rise to a semi-circle in the $Z^*(\omega)$ plane as those shown in Fig. 2.a (obtained for C_8MIMPF_6 and water-saturated/C_8MIMPF_6 systems); this semicircle has intercepts on the Z_{real} axis at R_∞ ($\omega \; –> \infty$) and R_o (ω –> 0), being (R_o-R_∞) the resistance of the system; the maximum of the semi-circle equals 0.5(R_o-R_∞) and occurs at such a frequency that $\omega RC=1$, being $\tau=RC$ the relaxation time [26]. A comparison of the semicircles presented in Fig. 2.a shows the strong effect of water on the electrical parameters associated the C_8MIMPF_6 ionic liquid, being the electrical resistance of the water-saturated/C_8MIMPF_6 approximately 30 % of that for the dry IL. Moreover, the data drawn in Fig. 2.b (impedance real part as a function of the frequency) also show differences in the liquid-electrode interface (f < 1000 Hz) between both systems.

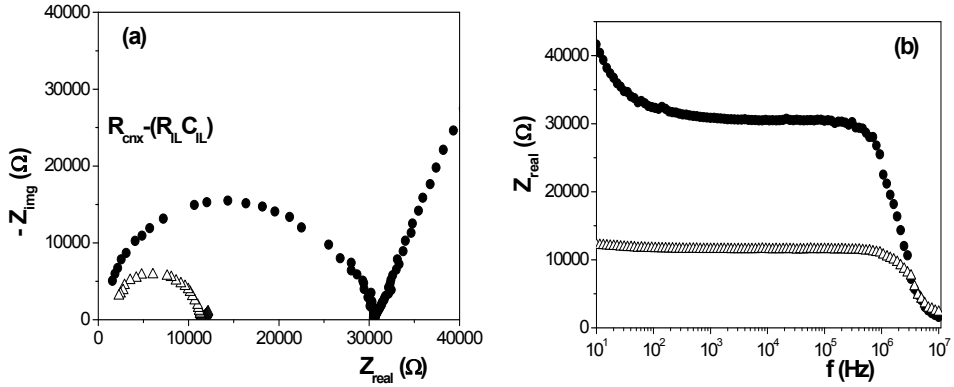

Fig. 2. Impedance plots for the ionic liquid C_8MIMPF_6 (●) and a water saturated mixture of C_8MIMPF_6 (Δ). (a) Nyquist and (b) Bode plots.

The reduction of the IL electrical resistance (or the conductivity increase) with water addition might be a point of interest for measurements carried out with ILs in electrochemical applications due to room humidity (open cells) or contact with aqueous solutions. According to Rivera-Rubero and Baldelli water is often present as a contaminant (up to ~ 0.2 mol fraction) in hydrophilic and hydrophobic ILs, highly affecting the bulk physical properties as well as the surface of hydrophobic ones [27]. In this context, it is interesting to remark the interfacial effects found when IS measurements at different time instances were performed with C_8MIMPF_6, in the open test-cell A and laboratory humidity of 50 %, shown in Fig. 3.a, where a new relaxation can be observed in the interfacial region ($f_{max} \approx 300$ Hz), but this effect hardly appears in measurements performed with test-cell B; in both cases bulk liquid contribution is practically unaffected. Results in Fig. 3.a could indicate that the electrodes also act as a pathway for water transport (no diffusion through the IL), which may cover the electrode measuring surface and, consequently, to modify the electrode/IL interface.

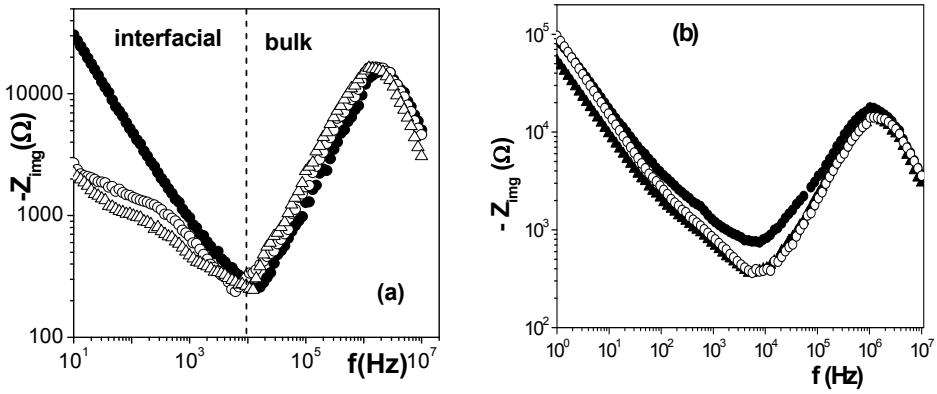

Fig. 3. Effect of water adsorption in the impedance plots measured for the RTIL C_8MIMPF_6 at different times: t = 0 h (●), t = 6 h (o) and t = 8 h (Δ). (a) in test-cell A; (b) in test-cell B.

To avoid that effect and clarify the electrical modifications caused by water diffusion into the IL, a more detailed study was performed by covering both free surfaces of the IL C_8MIMPF_6 with distilled water (measures carried out in test-cell B), and Fig. 4 shows time evolution of the impedance plots due to both water diffusion into the IL and water mixture/content. As can be observed, water diffusion (time evolution) seems to affect more to the real part of the impedance (Fig. 4.a) than the imaginary part (Fig. 4.b); however, water content modifies both real and imaginary impedance parts, shifting to higher frequencies the maximum frequency.

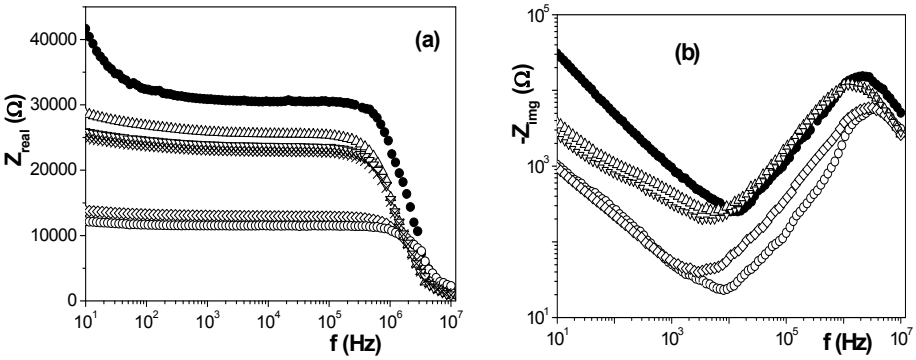

Fig. 4. Modification of impedance plots with water content in the ionic liquid C_8MIMPF_6. (●) no-water content, (Δ) 25 % of water on the IL surfaces (no-mixing) at t = 0 h and (∇) at t = 24 h; (x) 35 % of water on the IL surfaces (no-mixing) at t = 0, (◊) 35 % water mixture, (o) water saturated IL.

The fit of the impedance data using a non-linear program allows the determination of the electrical resistance of the ionic liquid C_8MIMPF_6 at different water content and the values are shown in Fig. 5.a; for comparison, results obtained with C_4MIMPF_6, another RTIL, are also indicated in Fig. 5.a [28]. These results show a direct relationship between the IL

electrical resistance and the size of the alkali chain and agree with lower conductivity of C_4MIMPF_6 when compared with C_8MIMPF_6 already reported in the literature [29]. Among other different physicochemical parameters of liquid systems, the viscosity and its dependence with water content is of higher interest. Measurements of $[C_8MIM][PF_6]$ at different water contents also showed a decrease of viscosity values with increasing water content [30], which is due to the reduction of the electrostatic attraction between the ions associated to the presence of the water molecules, lowering the energy of the system and, as a result of this, its viscosity. Combining the Stokes-Einstein equation for the diffusion coefficient of a particle with the Nernst-Einstein law for the total conductivity is possible to obtain a linear relationship between the electrical resistance and the apparent viscosity (η) for a particular IL [31], which allows the determination of η value for certain water content. Fig. 5.b shows the variation of apparent viscosity with water percentage for the ILs C_8MIMPF_6 and C_4MIMPF_6, where the lower viscosity of this latter can be observed [28].

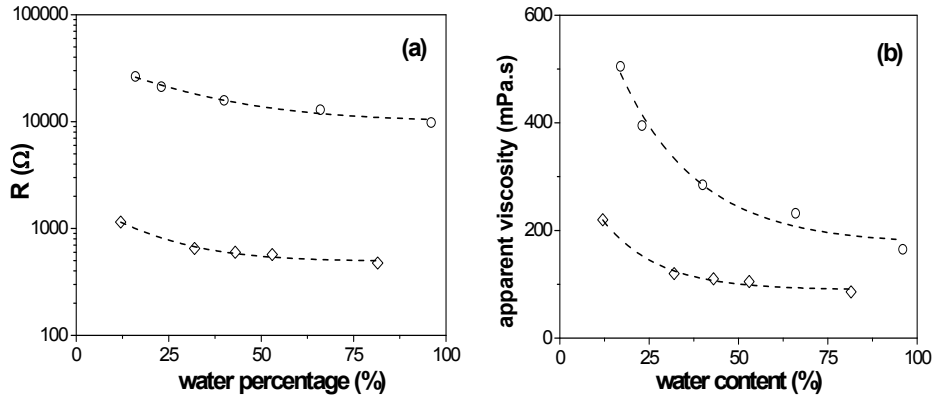

Fig. 5. Variation of C_8MIMPF_6 ionic liquid electrical resistance (a) and apparent viscosity (b) with water percentage (from ref. [28]).

Chemical characterization of $[C_4MIM^+][PF_6^-]$, $[C_8MIM^+][PF_6^-]$ and $[C_{10}MIM^+][BF_4^-]$ room temperature ionic liquids was carried out by X-ray photoelectron spectroscopy (XPS) analysis. XPS technique consists in the irradiation of a sample with X-rays under vacuum and the measure of the kinetic energy ($E_{kinetic}$) of the photoelectrons ejected from the sample's surface. The emitted electrons binding energy (B.E.) can be calculated as: $E_{binding} = E_{photon} - E_{kinetic}$, where E_{photon} is the energy of the X-ray incident radiation. Since the electrons of each chemical element have a characteristic B.E., it is possible to identify which elements are present in the surface sample (a thin layer of 30-50 Å) and their relative atomic concentration percentages, A. C. (%) (except hydrogen and helium). Additionally, it may also be possible to know the chemical state of the elements based on small shifts in the binding energies [10].

Table 1 shows the A.C. percentages of the characteristic RTILs elements found on the surface of the studied samples, but small percentages of other elements (silicon, oxygen,…) were also detected and attributed to impurities/environmental contamination [10,32]; particularly, a small percentage of oxygen (no included in Table 1) was also found in the three ILs which is associated to the presence of water due to their hygroscopic character.

Since the values shown in Table 1 correspond to relative percentages and, therefore, can not be easily compared between different samples, the ratio between the different elements detected is also presented, as well as the expected theoretical ratios (in brackets).

Ionic Liquid	%C	%F	%N	%P	C/F	N/P	F/P	F/N	C/P	C/N
$[C_4MIM][PF_6]$	48.2	30.0	9.8	5.4	1.6(1.3)	1.8 (2)	5.5 (6)	3.1 (3)	9.0 (8)	5.0 (4)
$[C_8MIM][PF_6]$	63.1	21.6	9.3	3.7	2.9 (2)	2.5 (2)	5.8 (6)	2.3 (3)	16.9 (12)	6.8 (6)
$[C_{10}MIM][BF_4]$	60.3	12.8	6.1	3.8	4.7(3.5)	1.6 (2)	3.3 (4)	2.1 (2)	15.7 (14)	9.9 (7)

Table 1. Surface composition by XPS analysis of the ionic liquids $[C_4MIM][PF_6]$, $[C_8MIM][PF_6]$ and $[C_{10}MIM][BF_4]$ (theoretical ratios in brackets).

Because the presence of external contaminants does not affect the ratios between the elements of interest, they will be used for comparison between the different ILs as well as with the theoretical ones. The N/P, F/P and F/N ratios found for the $[C_nMIM][PF_6]$ (n = 4 or 8) ionic liquids show good agreement with the theoretical ones, as well as the F/B and F/N ratios in the case of $[C_{10}MIM][BF_4]$, while the slightly higher differences obtained for C/F, C/P and C/N may be associated to carbon contamination.

A comparison of the carbon core level (C 1s) spectra obtained for the three RTILs is shown in Fig. 6, where two different peaks, at binding energies of 286.5 eV (assigned to carbons of the imidazolonium head) and 285.0 eV (assigned to the alkyl chain and adventitious carbon) can be observed; differences in the relative contributions of the two peaks seem to be dependent on the length of the RTILs' alkyls chain [22].

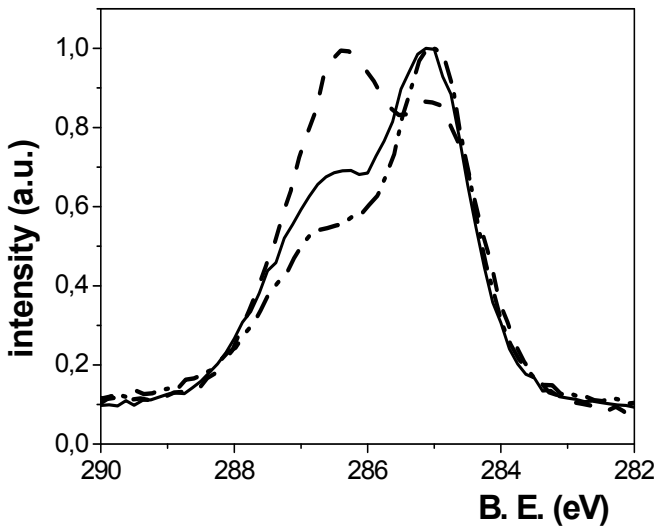

Fig. 6. C is core level spectra for the ionic liquids $[C_4MIM][PF_6]$ (solid line) $[C_8MIM][PF_6]$ (dashed line) and $[C_{10}MIM][BF_4]$ (dashed-dot line).

3.2 Electrical and chemical characteristics of membranes containing ionic liquids

Nowadays, membranes are used in different electrochemical applications and as was already indicated, the incorporation of room temperature ionic liquids into the membrane matrix may change its transport properties (mass/charge transport and selectivity) depending on the membrane structure and characteristics [1,33]. For that reason, changes in ion transport associated to the modification by ILs of porous and dense membranes are presented in this section.

3.2.1 Supported liquid membranes

Supported liquids membranes (SLMs) basically consist of an organic solvent immobilised in the pores of a support membrane [34]. SLMs has important transport advantages due to the high liquids diffusion rates and selectivity, but stability problems caused by the possible loss of the organic liquid from the porous support (or the formation of emulsions in the pores) have reduce their application in industrial separation processes [35-36]. Among the approaches suggested for improving SLMs stability, the use of RTILs as organic phase was also considered [28]. Among the different RTILs, those based in imidazolonium cation (1-n-alkyl-3-methylimidazolonium) seems to be particularly adequate due to their relatively high viscosity and reduced solubility for various solvents (including water), which are fundamental requirements for the durability of the organic phase of SLMs.

Chemical and electrical characterizations of a fresh SLM (sample *f*) and a 4 year old membrane stored without any special preservation procedure (sample *a*) were performed to see age effect on the structure and transport behaviour of the SLM (a porous PVDF matrix with pores filled with C_8MIMPF_6) [37].

A.C. (%) of the characteristic elements found on the surfaces of the porous PVDF support, and fresh (f) and aged (a) samples of the SLM containing $[C_8MIM^+][PF_6^-]$ into its pores are indicated in Table 2 (oxygen percentage and other impurities are not included, then total percentages differ from 100%). The coverage of the PVDF support by the IL is detected by a reduction in the percentage of fluorine and, more significant, the presence of phosphorous, an IL characteristic element, on the surface of the SLM fresh sample; however, the results obtained for the SLM aged sample show a slight increase of carbon (7 %) attributed to surface contamination, a reduction of 50 % in the A.C. of fluorine but an increase in the percentage of nitrogen and phosphorous, which might be taken as an indication of the re-organization of the IL rather than its lost.

Fig. 7.a shows the C 1s spectra for the PVDF-support, $[C_8MIM][PF_6]$ (f) and $[C_8MIM][PF_6]$ (a) samples. The two clear peaks showed by the PVDF support are ascribed to the $–CF_2–$ (at 291.2 eV) and the C* carbon in $CF_2–C^*H_2–$ bonds (at 286.7 eV due to the neighbourhood of the $–CF_2-$ group) [38]; moreover, a shoulder at 285.0 eV ascribed to adventitious carbon can also be observed, which support the slightly higher experimental C/F ratio obtained and indicated in Table 2. However, when fresh and aged SLM samples are compared, only slight differences associated to C=O bond (287.5 eV) attributed to membrane oxidation can be observed.

To ensure the presence of the IL not only on the membrane surface but also filling the pores of the aged sample, attenuated total reflectance Fourier transform infrared (ATR/FTIR) technique was used due that depth penetration of the infrared waves in this type of membranes is around 1.5 μm [39]. Fig. 7.b shows a comparison of the ATR-FTIR spectra in the range 3300-2800 cm^{-1} for the $[C_8MIM][PF_6]$ aged membrane and the PVDF support where the presence of the RTIL is clearly demonstrated by the appearance of the bands

assigned at imidazolium derivates when a comparison with the polymeric support is carried out; particularly, the absorption bands at 2928 and 2856 cm^{-1} correspond to asymmetric and symmetric stretching vibrations of methylene groups, and other bands assigned to asymmetric and symmetric stretching vibrations of methyl groups can also be appreciated at 2956 and 2873 cm^{-1} [37].

Membrane	C (%)	F (%)	N (%)	P (%)	C/F
PVDF support	54.1	41.9	0.9	---	1.29
$[C_8MIM^+][PF_6^-]$ (f)	57.4	24.1	3.7	2.5	2.38
$[C_8MIM^+][PF_6^-]$ (a)	61.5	10.5	6.9	4.0	5.86

Table 2. Atomic concentration percentage of the characteristic elements present on the surface of the PVDF support, $[C_8MIM^+][PF_6^-]$ fresh (f) and aged (a) RTIL supported membranes

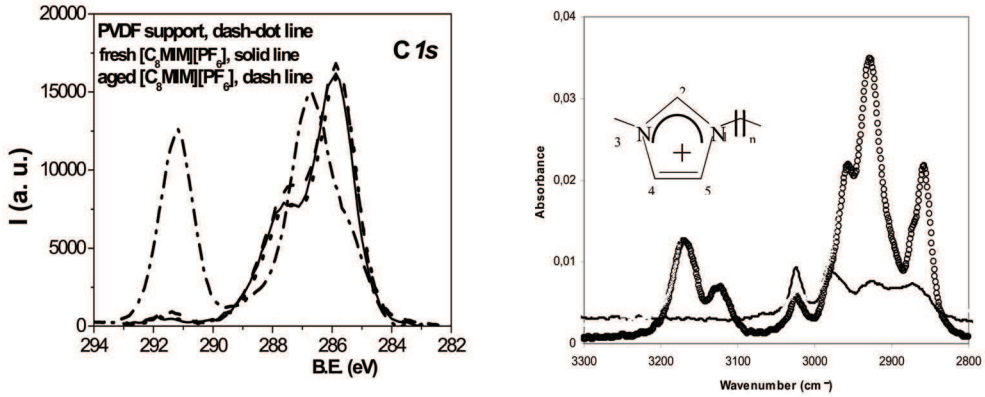

Fig. 7. (a) C1s core level spectra for $[C_8MIM][PF_6]$ fresh (solid line) and aged (dash line) membranes, and the PVDF porous support (dash-dot line). (b) ATR-FTIR spectra for aged $[C_8MIM][PF_6]$ SLM (o) and PVDF support (solid line).

Age effect on the transport across the SLM was determined by considering modification in the ion transport number (t_i), an electrochemical characteristic parameter which represents the ratio between the electric current transported by the ion *i* with respect to the total current crossing the membrane ($t_i = I_i/I_T$), then for single salts: $t_+ + t_- = 1$. Fig. 8.a shows a comparison of the electromotive force, ΔE_{med}, measured at both sides of fresh and aged SLM samples versus concentration ratio; rather similar ΔE_{med} values were obtained for both samples at low concentrations (c_v <0.02 M), but differences at high concentrations can be observed. Thermodynamic arguments lead to the following relationship between the electromotive force measured by the electrodes placed in the two half-cells, ΔE_{med}, the cation transport number, t_+, and the NaCl concentration of the solution filling each half-cell (c_1 and c_2) [40]:

$$\Delta E_{med} = -(2RT/F) \int_{c1}^{c2} t_+ \, dc \quad (2)$$

where R and F are gas and Faraday constants, T is the thermodynamic temperature of the system. For an ideal cation-exchange membrane ($t_+ = 1$), the ΔE_{med} reaches the maximum

value [40]: $\Delta E_{max} = - (2RT/F) \ln(c_2/c_1)$, and the cation transport number in the membrane for a given pair of solutions can be obtained as:

$$t_+ = \Delta E_{med}/\Delta E_{max} \quad (3)$$

Cation transport number across fresh and aged membranes were determined by using Eq. (3) and Fig. 8.b shows a comparison of t_+ values as a function of the NaCl average concentration ($<c_{NaCl}>=(c_1 + c_2)/2$) at the highest concentrations ($c_2 > 0.02$ M, most significant differences). As can be observed, a practically constant cation transport value ($<t_+> = (0.416 \pm 0.014)$) for the whole interval of concentration was obtained with the fresh sample, but t_+ values decrease with the increase of concentration for the aged sample. This result could be due to modification of the PVDF-RTILs interactions as a result of age, with could facilitate water (or NaCl aqueous solution) transport through the RTIL [37], although the partial lost of the RTIL from the pores of the aged membrane could also be considered. It should be remark that modification of Na^+ transport for the aged sample is only significant at high concentrations and, consequently, when a relatively high osmotic pressure is acting on the RTILs placed into the pores (between 1 and 4.5 bar), but the system is stable at lower pressures.

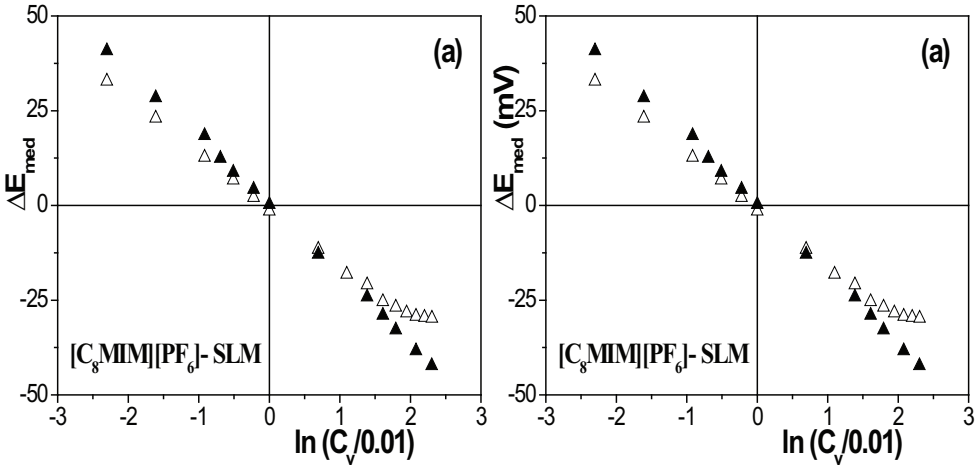

Fig. 8. (a) Variation of the measured potential at both membrane sides with NaCl concentration ratio; (b) Variation of cation transport number with NaCl average concentration. (▲) fresh $[C_8MIM][PF_6]$ membrane, (Δ) aged $[C_8MIM][PF_6]$ membrane.

3.2.2 Modification of dense membranes by inclusion of a IL or a IL-cation.

Two dense commercial polymeric membranes, a cation-exchange polytetrafluoroethylene backbone with sulfonic groups (Nafion) and a hydrophilic regenerated cellulose (RC), were modified with by inclusion of a IL-cation or a IL, respectively, into the polymer structure. Nafion membranes are widely used in electrochemical applications, mainly for fuel cell studies (PEMFCs) due to their good mechanical, chemical and thermal stability up to temperatures of 80 ºC, while cellulose and is derivatives are common membrane materials for different separation processes (hemodialysis, reverse osmosis, microfiltration,…) [6,41].

Although IL-modification of both dense membranes was performed by immersion of the samples in the IL or in an IL-water mixture, modification mechanism differs depending on the type of membrane. In the case of Nafion membranes the mechanism consists in the H^+/IL-cation exchange [20], while the IL-water mixture is embeded into the structure of the highly hydrophilic RC membrane.

Modification of the Nafion-protonated membrane was performed by immersion in a solution of the IL for a specific period of time and both conductivity and pH of the IL solution were measured at different time intervals [42]. The system presented in this paper correspond to n-dodecyltriethylammonium (DTA^+) which is solid at room temperature, and a 40% (w/w) IL aqueous solution with deionised water was prepared. These results showed an increase of DTA^+ incorporation along the time associated to the H^+/DTA^+ exchange, with a maximum value around 88 % at 20 h and a stable degree of incorporation percentage of 66 % between 24 h and 48 h [42].

Time evolution of IS measurements for the system *electrode/ DTA^+-water solution/ Nafion membrane/DAT^+-water solution /electrode* were carried out to monitory electrical changes in the Nafion membrane related with DTA^+ incorporation and Fig. 9.a shows the increase of the real part of the impedance (directly related to the electrical resistance) with time as a result of DTA^+ incorporation and, consequently, proton-content reduction; moreover, Z_{real} also presents higher values around 20 h (higher DTA^+ content) and a slight reduction and stabilization at higher contact times was also found in agreement with solution modification measurements previously indicated. XPS analysis of Nafion-protonated sample for different contact time with the DTA^+-water solution was also carried out and time evolution of the A.C. (%) for two characteristic elements, carbon and fluorine, is shown in Fig. 9.b. A decrease of fluorine A.C. (%) and an increase of carbon A.C. (%) with the increase of Nafion/IL-cation contact time can be observed. This is also a confirmation of the increase of DTA^+ incorporation into the Nafion structure.

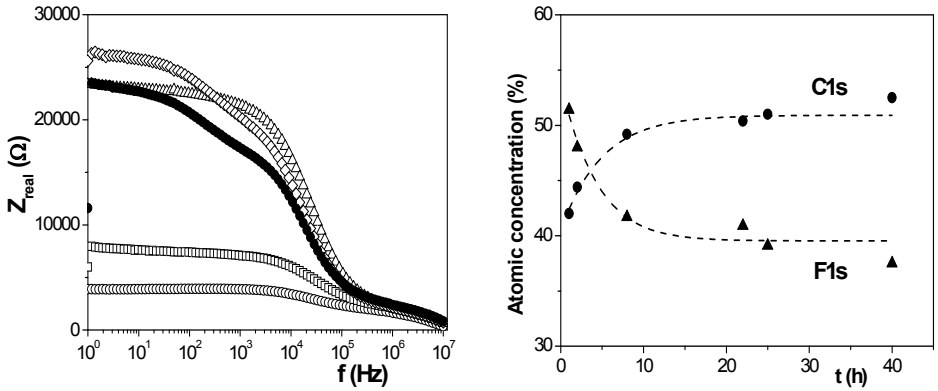

Fig. 9. (a) Time evolution of the Bode plot (Zreal vs frequency) for the Nafion membrane associated to the DTA^+ IL-cation incorporation by cation-exchange mechanism. (o) t = 0, (□) t = 1 h, (Δ) t = 6 h, (∇) t = 19 h, (◊) t = 26 h, (●) t = 40 h. (b) Time evolution of the carbon and fluorine atomic concentration percentages in the Nafion/DTA^+ system determined by XPS analysis.

Interfacial effect for the Nafion/DTA+-water solution system after a certain time of contact can also be observed if the - Z_{img} vs frequency plot is considered as is shown in Fig. 10.a. The impedance plot shows a new relaxation process in the interfacial region after 10 h of contact between the Nafion membrane and the DTA+-water solution [43], which might be related with the hydrophobic character of the polytetrafluoroethylene backbone of Nafion. To check this point, impedance measurements with the Nafion membrane immerse in the room temperature ionic liquid $BMIMBF_4$ (no water solution was necessary) at different times were also performed. No interfacial relaxation process was detected in this system as can be observed in Fig. 10.b. However, physicochemical differences between both cations could also be considered to explain the different electrical behaviour of both membrane systems.

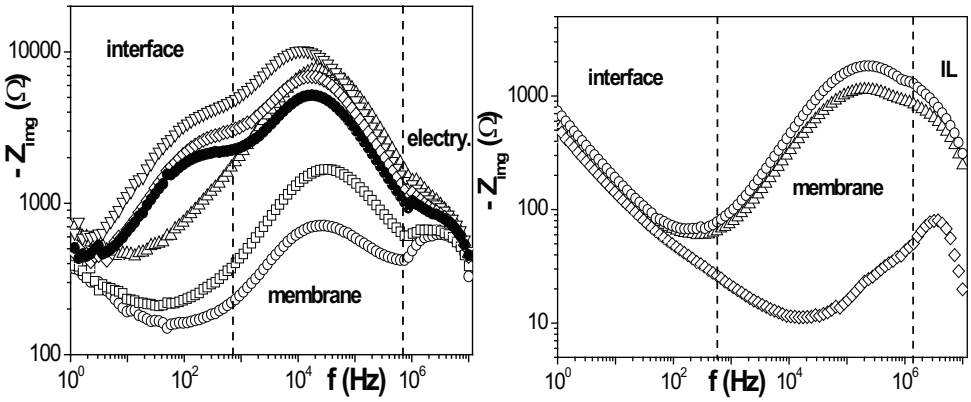

Fig. 10. (a) Time evolution of the Bode plot (- Zimg vs frequency) for the Nafion membrane associated to IL-cation incorporation. (a) Nafion/DTA+ system: (o) t = 0, (□) t = 1 h, (Δ) t = 6 h, (∇) t = 19 h, (◊) t = 26 h, (●) t = 40 h. (b); (b) Nafion/BMIM+ system: (□) t = 1 h, (Δ) t = 5 h, (◊) t = 20 h.

The small changes caused by the incorporation of BF_4^+ in the Nafion membrane and the reduction in water lost at temperatures higher than 100º C reported by Neves et al [42] makes of this RTIL a good candidate for inclusion in membranes with applications in low temperature fuel cells. In fact, these results have shown the possibility of electrical and chemical modifications of a typical commercial membrane for electrochemical applications with incorporation of ILs by ion-exchange mechanism, which strongly depend on the IL selected, opening a wide range of possibilities for particular membrane applications.

The inclusion of $BMIMBF_4$ in the structure of the regenerated cellulose RC-6 membrane and its effect on electrical and transport parameters was determined by comparing changes in electrical resistance and cation transport number determined with original and IL-modified membranes in contact with NaCl solutions at different concentrations (electrode/NaCl solution/membrane/NaCl solution/electrode system), moreover XPS analysis and IS measurements with dry samples were also performed for a more complete characterization. Fig. 11.a shows impedance plots (Z_{real} vs frequency and $-Z_{img}$ vs frequency plots) for RC-6 y

RC-6/BMIM membranes in contact with a 0.001 M NaCl solution, where clear differences between both samples can be observed. Since a unique relaxation process for the whole membrane system (membrane plus electrolyte placed between the membranes and the electrodes) was obtained, separate membrane characterization from IS measurement is not possible, but the results show higher values for the RC-6/BMIM membrane electrical resistance (Z_{real} vs f plot in the left axis of Fig. 11.a) and a shift to lower frequency in the - Z_{img} vs f plot (right axis in Fig. 11.a) associated to a denser structure [16], which seems to be caused by a reduction in the swelling degree of the cellulosic membrane as a result of the IL inclusion. Fig. 11.b shows the variation with the NaCl concentration of the membrane system electrical resistance (R_{ms}) determined from the analysis of the impedance data; the strong reduction for R_{ms} values with solution increase obtained is associated to the electrolyte-concentration dependence, but differences between RC-6 and RC-6/$BMIMBF_4$ membranes are only significant at low concentrations, since at high concentrations the charges in solution can screen the membrane electrical properties; however, higher capacitance values (around 18 %) were obtained for the RC-6/$BMIMBF_4$ membrane and whole interval of NaCl concentration.

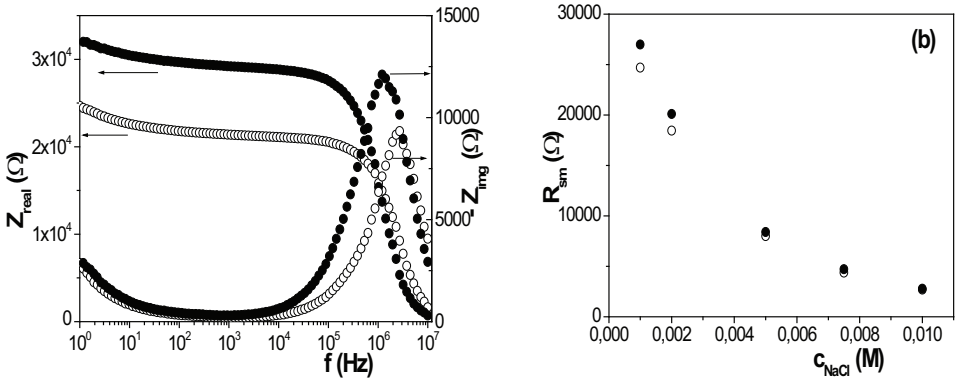

Fig. 11. (a) Impedance plots (Z_{real} vs f, left axis; - Z_{img} vs f, right axis). (b) Variation of the membrane system electrical resistance with NaCl concentration. (o) membrane RC-6/w, (●) membrane RC-6/$BMIMBF_4$.

However, dry samples show opposite behaviour as can be observed in Fig. 12 where Z_{real} vs frequency plots are compared. Since these measurements correspond to the system electrode/membrane/electrode, R_m values for the (dry) membrane matrix are obtained from these measurements (no electrolyte exists), which allows the determination of the membrane conductivity, a material characteristic parameter: $\sigma_m = \Delta x_m/S_m.R_m$, where S_m and Δx_m represent the membrane area and thickness, respectively. The following values were obtained:

RC-6 membrane: $\sigma_m = 1.0x10^{-5}$ $(\Omega.m)^{-1}$.

RC-6/$BMIM^+$ membrane: $\sigma_m = 1.8x10^{-3}$ $(\Omega.m)^{-1}$.

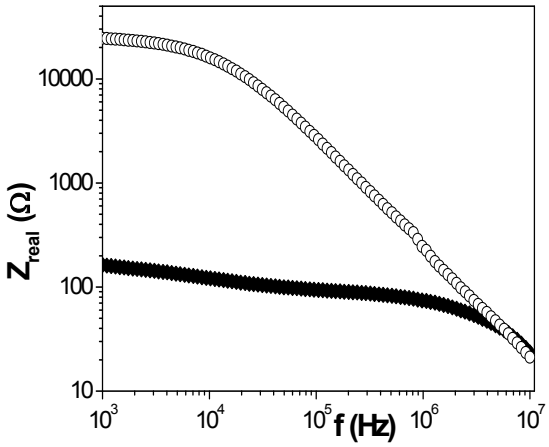

Fig. 12. A comparison of Z_{real} versus frequency plot for dry RC-6 (◊) and RC-6/BMIMBF$_4$ (♦) membranes.

According to these results, the presence of the ionic liquid BMIMBF$_4$ impregnating the free space among the cellulose chains in the solid matrix significantly increases the membrane conductivity.

The membrane impregnation assumption is supported by the values obtained from the XPS analysis carried out at different take off angles according to the A.C. (%) determined, which are indicated in Table 3. These results show and increase in fluorine and nitrogen, both IL elements, in the RC-6/BMIMBF$_4$ membrane with the increase of the take off angle, that is, when a deeper analysis is carried out.

	RC-6/w					RC-6/BMIMBF$_4$				
Φ (°)	C 1s (%)	O 1s (%)	Si 2p (%)	N 1s (%)		C 1s (%)	O 1s (%)	Si 2p (%)	N 1s (%)	F 1s (%)
20	62.9	19.9	16.9	0.3		65.1	28.1	4.1	1.2	1.5
45	64.0	20.2	15.3	0.5		61.9	32.8	2.4	1.4	1.5
75	65.4	20.9	13.1	0.6		62.4	32.3	1.8	1.7	1.9

Table 3. Atomic concentration percentages of the elements found on the surfaces of the RC-6/w and RC-6/LL membranes at different take off angles (Φ)

The effect of IL on the ion transport was also determined from membrane potential measurements and Fig. 13.a shows the membrane potential for RC-6/w and RC-6/BMIMBF$_4$ samples as a function of the ratio of the NaCl solution concentrations at both membrane sides. For NaCl concentrations lower than 0.01 M membrane potentials for both membranes are very similar and they slightly differ from the values associated to an ideal cation-exchange membrane, but clear differences are obtained at higher concentrations (0.02

$M \leq C_{NaCl} \leq 0.2$ M). This behaviour is common for weak charged membranes [25,41] and is associated to the Donnan co-ion exclusion at low concentrations (when the solution concentration is lower than the effective membrane fixed concentration), but this effect is practically neglected at high solution concentrations, when the number of solution charges are able to screen membrane fixed charge, and the membrane potential mainly corresponds to a diffusion potential due to the different mobility of Na^+ and Cl^- in the membrane.

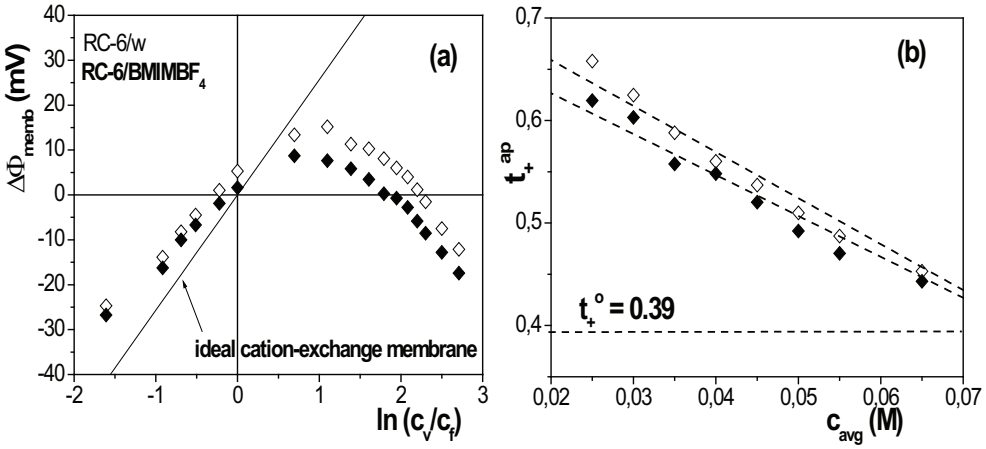

Fig. 13. (a) membrane potential vs NaCl concentration ratio. (b) Apparent cation transport number vs average NaCl concentration. (◊) membrane RC-6/w, (♦) membrane RC-6/$BMIMBF_4$.

Cation transport number across RC-6/w and RC-6/$BMIMBF_4$ membranes was determined by Eq. (3) and Fig. 13.b shows its variation with the average concentration ($c_{avg} = (c_v + c_c)/2$) for both membranes. Cation transport numbers determined by Eq. (2) are usually named "apparent transport number", t_+^{ap}, since water transport is not considered, which is a rather good approximation for most dense membranes, but it can slightly differ from true membrane transport number, t_+^m, in the case of highly hydrophilic membranes as the RC samples. Scatchard obtained the following relationship between both apparent and true cation transport numbers in a membrane [44]:

$$t_+^{ap} = t_+^m - 0.0018\, t_w\, (C_{avg}) \quad (4)$$

where t_w represent the water transport number. From the slopes of the straight lines shown in Fig. 13.b, taking into account Eq. (4), the following values for t_+^m and t_w in RC-6/w and RC-6/LL membranes were obtained:

membrane RC-6/w: $t_+^m = 0.66 \pm 0.02$, $t_w = 255 \pm 15$

membrane RC-6/$BMIMBF_4$: $t_+^m = 0.62 \pm 0.02$, $t_w = 220 \pm 12$

These results show a reduction of 6 % in the transport of Na^+ ions and 14 % in the water transport associated as a result of the presence of the $BMIMBF_4$ ionic liquid.
To check that result, water diffusion measurements were performed using tritied water with a given activity (A_f) at one side of the membrane (donor chamber) and distilled water at the other membrane side (receiving chamber) [25, 45]. Taking into account the mass continuity: $A_f^o = A_f^t + A_r^t$ = cte, where A_f^o is the initial activity of tritiaed water in the donor chamber (t = 0) while A_f^t and A_r^t the water activities in donor and receiving chambers at time t, the following expression is obtained [46]:

$$\ln([1 - (2A_r/A_f)] = - 2[S/(V_o.\Delta x)].P_w.t \quad (5)$$

where V_o and P_w are the chamber volume and water permeability, respectively. Fig. 14 shows variation of solutions activities with time, and P_w value for each membrane was obtained from the slopes of those straight-lines by using Eq. (4). Water diffusion coefficient was obtained by [41]: $D_w = P_w.\Delta x_m$, and the following values were obtained: $D_w^{RC\text{-}6/w} = 2.1x10^{-10}$ m²/s and $D_w^{mRC\text{-}6/LL} = 1.7x10^{-10}$ m²/s, which indicates a reduction of 15 % in water diffusion from direct measurements. This result agrees with those previously obtained and confirms a diminution of the free space among the cellulose chains associated to the presence of the IL, reducing the transport of both water and ions through the IL-modified cellulosic membrane.

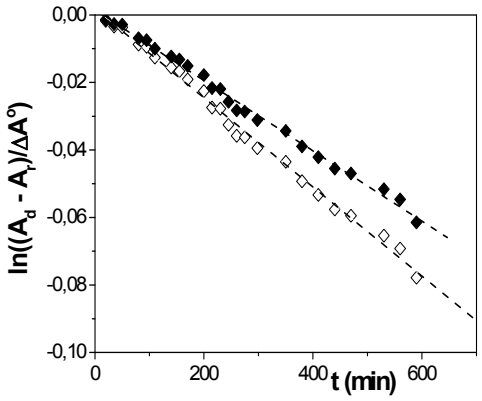

Fig. 14. Variation of tritiaed water activity in donor and receiving chambers as a function of time for RC-6/w (◊) and RC-6/$BMIMBF_4$ (♦) membranes.

Moreover, these results show the possibility of easy membrane modification by its immersion in an IL-water solution, which hardly modifies the transport of ions across the original membrane but reduces the mass transport, which is a requirement of interest for energy applications of membranes (reduction of cross flow in fuel cells) and electrochemical devices.

4. Conclusions

Electrical and chemical surface characterizations of different imidazolonium-bases RTILs carried out by impedance spectroscopy and XPS measurements was presented. The reduction in the electrical resistance of the ILs the increase of water content were correlated with the reduction in viscosity of the ILs.

The modification of various kinds of polymeric membranes, with different structures (porous and dense), materials (PVDF, RC and Nafion) and process applications (filtration, dialysis and electrodialysis), by inclusion of ILs in the pores as organic phase of supported liquid membranes or into the structure of dense samples (by ion-exchange or embeded into the membrane matrix) and its effect on transport parameters was also presented. The variety of ILs made possible to choose that more adequate for a specific membrane process, which opens its use in a wide variety of applications, particularly related to electrochemical systems.

5. Acknowledgements

We thank to Comisión Interministerial de Ciencia y Tecnología (CICYT, Project MAT/2007-65065, Spain) for financial support.

6. References

[1] M. Armandi, F. Endres, D.R. MacFarlane, H. Ohno, B. Scrosati; *Nature Materials*, 8 (2009) 621.

[2] J.F. Brennecke, E.J. Magin; *AICHEJ*, 47 (2001) 2384.

[3] J.D. Figueroa, T. Fout, S. Plasynski, H. McIlvried, R.D. Srivastava; *Int. J. Greenhouse Control*, 2 (2008) 9.

[4] J. Ranke, S. Stolte, R. Strmann, J. Arning, B. Jastorff; *Chemical Reviews*, 107 (2007) 2183.

[5] K. Yuyama, G. Masuda, H. Yoshida, T. Sato; *J. Power Sources*, 162 (2006) 1401.

[6] V. S. Silva, B. Ruffmann, S. Vetter, M. Boaventura, A. M. Mendes, L. M. Madeira, S. P. Nunes; *Electrochimica Acta*, 51 (2006) 79.

[7] M. Doyle, S. Choi, G. Proulx; *J. Electrochem. Soc*., 147 (2000) 34.

[8] C. Schmidt, T. Glück, G. Schmidt-Naake; *Chem. Eng. Technol*., 31 (2008) 13.

[9] D. Susac, M. Kono, K.C. Wong, K.A.R. Mitchell; *Appl. Surf. Sci*. 174 (2001) 43.

[10] M. J. Ariza, J. Benavente, E. Rodríguez-Castellón; in "Handbook of Membranes: Properties, Performance and Applications" (Ed. S. V. Gorley). Nova Science Publishers, Inc., New York, 2009.

[11] R. Fortunato, C.A.M. Afonso, J. Benavente, E. Rodriguez-Castellón, J.G. Crespo; *J. Membr. Sci*., 256 (2005) 216.

[12] K. Sakai; *J. Membr. Sci*., 96 (1994) 91.

[13] J. Mijovíc, F. Bellucci; *Trends in Polym. Sci*., 4 (1996) 74.

[14] J. Benavente, J.M. García, R. Riley, A.E. Lozano, J. de Abajo; *J. Membr. Sci*., 175 (2000) 43.

[15] V. Compañ, E. Riande, F.J. Fernandez-Carretero, N.P. Berezina, A.A.-R. Sytcheva; *J. Membr. Sci*., 318 (2008) 255.

[16] J. Benavente; Electrical Characterization of Membranes, in Monitoring and Visualizing Membrane-Based Process, Eds. C. Güell, M. Ferrando, F. López. Wiley-VCH, 2009.
[17] P.A.Z. Suarez, J.E.L. Dullius, S. Einloft, R.F. de Sousa, J. Dupont; *Polyhedron*, 15(7) (1996) 1217.
[18] J.D. Holbrey, K.R. Seddon; J. Chem. Soc., *Dalton Trans*., 13 (1999), 2133.
[19] A.E. Visser, R.P. Swatloski, R.D. Rogers; *Green Chemistry*, 2 (2000) 1.
[20] T. Schäfer, R. E. Di Paolo, R. Franco, J. G. Crespo; *Chemical Communications* (2005) 2594.
[21] D. Brigg, M. P. Seah; Practical Surface Analysis: Auger and X-Ray Photoelectron Spectroscopy, vol.1, 2º ed., John Wiley & Sons, Chichester, 1995.
[22] J. F. Moulder, W. F. Stickle, P. E. Sobol, K. D. Bomben; Handbook of X-Ray Photoelectron Spectroscopy, ed. J. Chastain. Perkin-Elmer Corporation, Minneapolis, 1992.
[23] M.J. Ariza, P. Prádanos, R. Rico, E. Rodriguez-Castellón, J. Benavente; *Surf. Interface Anal*., 35 (2003) 360.
[24] R. de Lara, M.I. Vázquez, P. Galán, J. Benavente; *J. Membr. Sci*., 273 (2006) 25.
[25] J.D. Ramos, C. Milano, V. Romero, S. Escalera, M.C. Alba, M.I. Vázquez, J. Benavente; *J. Membr. Sci*., 352 (2010) 153.
[26] J.R. Macdonals; *Impedance Spectroscopy*, Wiley, New York, 1987.
[27] S. Rivera-Rubero, S. Baldelli; *J. Am. Chem. Soc*., 126 (2004) 11788.
[28] R. Fortunato, L.C. Branco, C.A.M. Afonso, J. Benavente, J.G. Crespo; *J. Membr. Sci*., 270 (2006) 42.
[29] D.L. Compton, J.A. Laszlo; *J. Electroanal. Chem*., 520 (2002) 71.
[30] R. Fortunato, C.A.M. Afonso, M.A. Reis, J.G. Crespo; *J. Membr. Sci*., 242 (2004) 197.
[31] K.B. Oldham, J.C. Myland; Fundamental of Electrochemical Science, Academic Press Incorporated, 2004.
[32] J.T.F. Keurentjes, J.G. Harbrecht, D. Brikman, H.H. Hanemaaijer, M.A. Cohen, H. van´t Riet; *J. Membr. Sci*., 47 (1989) 333.
[33] L.A. Neves, I.M. Coelhoso, J.G. Crespo; *J. Membr. Sci*., 360 (2010) 363.
[34] M.Oleinikova, M.Muñoz, J.Benavente, M.Valiente; *Langmuir*, 16(2) (2000) 716.
[35] P. Scovazzo, J. Kieft, D.A. Finah, C. Koval, D. DuBois, R. Noble; *J. Membr Sci*., 238 (2004) 57.
[36] E. Miyako, T. Maruyama, N. Kamiya, M. Goto; *Chem. Commun*., 23 (2003) 2926.
[37] S. Bijani, R. Fortunato, M.V. Martínez de Yuso, F. A. Heredia-Guerrero, E. Rodríguez-Castellón, I. Coheloso, J. Crespo, J. Benavente; *Vacuum*, 83 (2009) 1283.
[38] M.D. Duca, C.L. Plosceanu, T.J. Pop; *Appl Polym Sci*., 67 (1998) 2125.
[39] Y. Jeon, J. Sung, C. Seo, H. Lim, H. Cheong, M. Kang, B. Moon, Y. Ouchi, D.J. Kim; *J. Phys. Chem. B*, 112 (2008) 4735.
[40] F. G. Helfferich; Ion Exchange, McGraw-Hill Book Company, New York, 1962.
[41] M. Mulder, Basic Principles of Membrane Technology, Kluwer Acad. Publishers, Dordrecht, The Netherland, 1992.
[42] L. Neves, J. Benavente, I.M. Coelhoso, J.G. Crespo; *J. Membr. Sci*., 347 (2010) 42.
[43] J. Benavente, L. Neves, I. Coelhoso, J.G. Crespo; 2º Interface and Colloid Iberic Conference. Coimbra (Portugal), 2007.
[44] G.J. Scartchard; *J. Amer. Chem. Soc*., 75 (1953) 2883.

[45] S. Escalera, S. Bijani, P. Galán, J. Benavente; XI Congreso Nacional de Materiales, Zaragoza (Spain), 2010.
[46] D.L. Gilbert, T. Okano, T. Miyata, S.W. Kim; *Int. J. Pharm*., 47 (1988) 79.

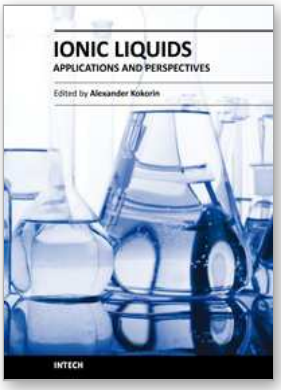

Ionic Liquids: Applications and Perspectives

Edited by Prof. Alexander Kokorin

ISBN 978-953-307-248-7
Hard cover, 674 pages
Publisher InTech
Published online 21, February, 2011
Published in print edition February, 2011

This book is the second in the series of publications in this field by this publisher, and contains a number of latest research developments on ionic liquids (ILs). This promising new area has received a lot of attention during the last 20 years. Readers will find 30 chapters collected in 6 sections on recent applications of ILs in polymer sciences, material chemistry, catalysis, nanotechnology, biotechnology and electrochemical applications. The authors of each chapter are scientists and technologists from different countries with strong expertise in their respective fields. You will be able to perceive a trend analysis and examine recent developments in different areas of ILs chemistry and technologies. The book should help in systematization of knowledges in ILs science, creation of new approaches in this field and further promotion of ILs technologies for the future.

InTech Europe
University Campus STeP Ri
Slavka Krautzeka 83/A
51000 Rijeka, Croatia
Phone: +385 (51) 770 447
Fax: +385 (51) 686 166
www.intechopen.com

InTech China
Unit 405, Office Block, Hotel Equatorial Shanghai
No.65, Yan An Road (West), Shanghai, 200040, China
中国上海市延安西路65号上海国际贵都大饭店办公楼405单元
Phone: +86-21-62489820
Fax: +86-21-62489821